

Elastic and rotational excitation of the oxygen molecule by intermediate-energy electrons

P. K. Bhattacharyya

Department of Physics, Calcutta University, 92 Acharyya Prafulla Chandra Road, Calcutta 700009, India

K. K. Goswami

Department of Physics, Rishi Bankim Chandra College Naihati, 24 Parganas, West Bengal, India

(Received 6 July 1982)

The Glauber-type eikonal amplitude for a fixed molecular orientation is used in the framework of adiabatic approximation to compute pure elastic excitation ($J=1 \rightarrow J'=1$), rotational excitation ($J=1 \rightarrow J'=3$), and orientationally averaged elastic cross sections of the oxygen molecule in its ground electronic and vibrational states with the use of electrons as incident particles. Both differential and integral cross sections are reported at electron energies 20–200 eV. The effect of target polarization is included in the effective electron-molecule potential used, but that of electron exchange is neglected. The results are compared with the available experimental data and theoretical calculations of other workers. A comparative study of the molecules H_2 , N_2 , and O_2 as targets is made.

I. INTRODUCTION

During the last decade the problem of electron-molecule collision processes has received considerable attention^{1–4} because of the growing applications of these processes in diverse fields, such as electron lasers, planetary atmosphere, or the interstellar medium of outer space. Molecular oxygen is a major constituent of the Earth's atmosphere and plays an important role in slowing down the energetic electrons by collisions. It is well known that at low energy the rotational excitation of molecules is a dominant energy-loss mechanism; even at intermediate energy the rotational-excitation cross sections are found⁵ to be quite significant. However the elastic scattering and rotational excitation of oxygen molecules by electron impact have not been as well studied, either theoretically or experimentally, as those of nitrogen molecules,⁶ the other major constituent of the atmosphere. Fisk⁷ studied theoretically the elastic $e-O_2$ scattering problem based on an electron-molecule interaction which made the wave equation separable in two-center spheroidal coordinates. Using the potential of Fisk, which is short range in nature, Oksyuk⁸ applied the adiabatic approximation to investigate the rotational excitation of this molecule. The low-energy rotational excitation was also studied by Takayanagi,⁹ using the first Born approximation, and by Sampson and Mjolsness¹⁰ and by Geltman and Takayanagi¹¹ using the distorted-wave approximation. In these calculations the long-range part of the electron-molecule interactions was considered. Recently, the modified effective-range theory has been applied by Chang¹²

to study the elastic scattering at very low energies. At intermediate and high energies the only available calculations were those of Wedde and Strand¹³ and of Hayashi.¹⁴ These authors used the independent atom approximation and computed only the elastic (rotationally summed) scattering cross sections. Corrections due to electron-exchange and polarization of the target were neglected by Wedde and Strand, while the effect of polarization was considered by Hayashi. In his calculation of total scattering cross sections for electron-oxygen scattering Myers¹⁵ estimated the contributions of elastic as well as rotational-excitation cross sections. The earliest measurements reported on electron-oxygen-molecule scattering were those of Brüche¹⁶ and of Ramsaur and Kollath.¹⁷ Recently, elastic differential scattering cross sections have been measured by Trajmar *et al.*¹⁸ in the angular range 10° – 90° at energy interval 4–45 eV, by Bromberg¹⁹ between 2° and 40° and at 300–500 eV, by Hayashi¹⁴ between 10° and 60° and at 100–500 eV, and by Wakiya²⁰ between 5° and 130° and at 20–500 eV. Total scattering cross sections at 0.5–100 eV were measured by Sunshine *et al.*²¹ Apart from these, swarm-experiment data by Phelps and co-workers²² were available at the thermal energy region.

In the present paper we have studied the elastic scattering and rotational excitation of molecular oxygen by (20–200)-eV electron impact using the Glauber approximation.²³ This investigation is a continuation of our earlier works on homonuclear molecular targets, hydrogen^{24–26} and nitrogen,⁶ using a formulation of the Glauber approximation originally developed by Bhattacharyya and Ghosh.^{24,25}

Here a brief survey of the Glauber approximation as applied to molecular targets might be of interest. In recent years the Glauber approximation has become an effective tool for studying the electron-atom collision processes,²⁷⁻³³ particularly at intermediate energies. In comparison to electron-atom scattering, this approximation is less exploited in investigating the electron-molecule scattering because of the multicenter nature of the problem. Yates and Tenney³⁴ first applied the Glauber approximation to elastic scattering of high-energy electrons by molecular targets N₂, I₂, and U₂. The extension of this approximation to elastic scattering and inelastic processes at intermediate energies was initiated by Chang *et al.*³⁵ and by Bhattacharyya and Ghosh.²⁴⁻²⁵ Chang *et al.* studied the vibrational excitation of the hydrogen molecule, while Bhattacharyya and Ghosh^{24,25} and Bhattacharyya *et al.*²⁶ studied the elastic scattering and rotational excitation of the same molecule. Low-energy rotational excitation of polar molecules was investigated by Ashihara *et al.*³⁶ In these applications of the Glauber approximation only Bhattacharyya and Ghosh, and Bhattacharyya *et al.* considered the most realistic electron-molecule potential, which includes the contributions of static, polarization, and exchange interactions. Subsequently, elastic scattering cross sections for hydrogen molecules were computed by Huang and Chan³⁷ and by Gien³⁸ within the framework of independent scattering centers. Rotational-excitation cross sections for a few linear molecules were calculated by Gianturco and co-workers³⁹ considering only the asymptotic parts of the electron-molecule potential. LaGattuta⁴⁰ made an interesting study on rotational and vibrational excitations of hydrogen molecules. He introduced a Gaussian basis for the electronic part of the target wave function and was able to compute scattering cross sections without recourse to any model potential. Recently, Bhattacharyya and Goswami⁶ have calculated elastic and rotational-excitation cross sections for *e*-N₂ scattering, and these are found to agree well with those obtained by using sophisticated close-coupling approximation.⁴¹

For the effective electron-oxygen-molecule potential we have considered in the present calculation the polarization potential in addition to static potential. The effects of electron exchange are neglected. Cross sections for the elastic process $J=1 \rightarrow J'=1$, rotational-excitation process $J=1 \rightarrow J'=3$, and orientationally averaged elastic scattering are computed. A comparative study of the molecular targets H₂, N₂, and O₂ is made for the sake of completeness of our investigation on electron-homonuclear-diatomic-molecule scattering using the present method.

II. EFFECTIVE POTENTIAL AND THEORY

The effective electron-molecule potential $V(\vec{r}, \hat{R})$ can be written as

$$V(\vec{r}, \hat{R}) = V_s(\vec{r}, \hat{R}) + V_{\text{ex}}(\vec{r}, \hat{R}) + V_p(\vec{r}, \hat{R}), \quad (1)$$

where $V_s(\vec{r}, \hat{R})$ is the electrostatic interaction between the electron and the unperturbed ground-electronic charge distribution, $V_{\text{ex}}(\vec{r}, \hat{R})$ is the effective local potential which takes into account the effect of electron-exchange, and $V_p(\vec{r}, \hat{R})$ is the polarization potential which represents the effects of distortion of the target. \vec{r} is the position vector of the scattered electron measured from the center of mass of the molecule, and \hat{R} denotes the unit vector along \vec{R} , R being the internuclear separation at equilibrium. We expand $V(\vec{r}, \hat{R})$ in terms of Legendre polynomials,

$$V(\vec{r}, \hat{R}) = \sum_{\nu=0} V^{\nu}(r) P_{\nu}(\hat{r} \cdot \hat{R}). \quad (2)$$

The one-center expression (2) is slowly convergent near the nuclei, and a large number of terms is needed to represent the effective potential properly. Here we consider the first two terms in Eq. (2). With the use of Eq. (1) the coefficients of these terms become

$$\begin{aligned} V^0(r) &= V_s^0(r) + V_{\text{ex}}^0(r) + V_p^0(r), \\ V^2(r) &= V_s^2(r) + V_{\text{ex}}^2(r) + V_p^2(r). \end{aligned} \quad (3)$$

At large r , $V_s^2(r)$, $V_p^0(r)$, and $V_p^2(r)$ should behave as

$$\begin{aligned} V_s^2(r) &\underset{r \rightarrow \infty}{\sim} -Q/r^3, \\ V_p^0(r) &\underset{r \rightarrow \infty}{\sim} -\alpha_0/2r^4, \end{aligned} \quad (4)$$

and

$$V_p^2(r) \underset{r \rightarrow \infty}{\sim} -\alpha_2/2r^4,$$

where Q , α_0 , and α_2 are, respectively, the quadrupole moment, spherical, and nonspherical parts of the static dipole moment. But the small- r behavior of the long-range potentials $V_p^0(r)$ and $V_p^2(r)$ is not known accurately.⁴² For that reason, usually a cutoff function⁴² $f_c(r, r_c)$ with some adjustable parameter r_c is used to make these potentials well behaved at the center of mass of the molecule and to reproduce the cross sections as accurately as possible. In the present paper we have used the following form of the cutoff function:

$$f_c(r, r_c) = 1 - \exp[-(r/r_c)^6], \quad (5)$$

such that

$$\begin{aligned} V_p^0(r) &= -\frac{\alpha_0}{2r^4} f_c(r, r_c), \\ V_p^2(r) &= -\frac{\alpha_2}{2r^4} f_c(r, r_c), \quad \text{for all } r. \end{aligned} \quad (6)$$

α_0 and α_2 are taken⁴³ to be equal to $10.8e^2a_0^3$ and $4.95e^2a_0^3$, respectively. For many electron targets $V_s^0(r)$ and $V_s^2(r)$ can be calculated using the *ab initio* molecular wave functions^{44,45} or semiempirical molecular orbitals.⁴⁵ No such calculation is available for oxygen molecules. We have obtained¹ them by expanding the atomic potentials⁴⁶ in terms of Legendre polynomials [Eq. (11), Ref. 47] with the equilibrium internuclear separation $R=2.26a_0$. $V_s^2(r)$ so obtained does not reproduce the quadrupole tail properly; we have modified it by using the expression

$$-\frac{Q}{r^3} f_c(r, r_c),$$

Q being taken as the experimental quadrupole moment $(-0.29e^2a_0^2)^1$ of molecular oxygen. We call this potential model B. The potential model A will be defined in Sec. III A. Because of the similarity between oxygen and nitrogen molecules we have used the same cutoff parameter $r_c=2a_0$ as was used by us for nitrogen molecules.⁶ To show the depen-

$$\begin{aligned} I(J \rightarrow J', \theta) &= \frac{k_i^2(2J'+1)}{4} \sum_{M=-J}^J \sum_{M'=-J'}^{J'} \left| \left[\frac{(J-|M|)! (J'-|M'|)!}{(J+|M|)! (J'+|M'|)!} \right]^{1/2} \right. \\ &\quad \left. \times \int P_J^{|M|}(\cos\theta_m) f_{2n,n}(\theta, \theta_m) P_{J'}^{|M'|}(\cos\theta_m) \sin\theta_m d\theta_m \right|^2, \end{aligned} \quad (8)$$

and

$$\langle I(\theta) \rangle = \frac{k_i^2}{2} \sum_{n=0}^J \int \lambda_n f_{2n,n}^2(\theta, \theta_m) \sin\theta_m d\theta_m, \quad (9)$$

where $2n = |M - M'|$. Total cross section $\sigma(J \rightarrow J')$ for the transition $J \rightarrow J'$ or the average total cross section $\langle \sigma \rangle$ can be computed using Eqs. (8) or (9) in

$$\sigma = 2\pi \int_0^\pi I(\theta) \sin\theta d\theta. \quad (10)$$

It should be noted that average cross sections $\langle I(\theta) \rangle$ and $\langle \sigma \rangle$ include all the possible final rotational states for any initial rotational state J of the target molecule. For O_2 , only odd J 's are allowed since the electronic ground state is a triplet state (the coupling between the resultant electronic spin and

dence of cross sections on the cutoff parameter we have also computed all cross sections with $r_c=1.7a_0$. Recently, a number of model exchange potentials $V_{\text{ex}}(\vec{r}, \hat{R})$ for electron-molecule scattering has been tried by different workers.⁴⁸ We have however neglected the exchange potential in our calculations.

Using the expressions (2) and (3) for the effective electron-molecule potential the Glauber scattering amplitude $f(\theta, \hat{R})$ for a fixed orientation (θ_m, ϕ_m) of the molecular axis \vec{R} can be written as²⁵ (atomic units are used in the present paper)

$$f(\theta, \hat{R}) = -ik_i \sum_{n=0}^{\infty} i^n \lambda_n f_{2n,n}(\theta, \theta_m) \cos 2n\phi_m, \quad (7)$$

with

$$\lambda_n = \begin{cases} 1 & \text{for } n=0, \\ 2 & \text{for } n \neq 0, \end{cases}$$

where θ is the scattering angle and \vec{k}_i is the incident momentum. $f_{2n,n}$'s are defined elsewhere.^{6,25,26} In the derivation of Eq. (7) the polar axis is taken in the direction of \vec{k}_i . The amplitude (7) is used to derive²⁵ the differential scattering cross section $I(J \rightarrow J', \theta)$ for the excitation process $J \rightarrow J'$ and the average elastic differential scattering cross section $\langle I(\theta) \rangle$ using the adiabatic approximation^{1,8}

rotational motion is neglected because of its negligible effects on cross sections¹¹). In a previous article⁶ we described in detail the numerical procedure used by us to compute the cross sections [Eqs. (8)–(10)].

III. RESULTS AND DISCUSSIONS

In the present paper we have calculated the state-to-state differential scattering cross sections (DCS) $I(J \rightarrow J', \theta)$ and total scattering cross sections (TCS) $\sigma(J \rightarrow J')$ for the pure elastic process $J=1 \rightarrow J'=1$ and rotational-excitation process $J=1 \rightarrow J'=3$ at incident electron energies 20–200 eV. Within the same energy interval we have also computed the orientationally averaged elastic DCS $\langle I(\theta) \rangle$ and TCS $\langle \sigma \rangle$ as well as momentum transfer cross sections $\langle \sigma_m \rangle$. To study the dependence of these cross sections on the adjustable parameter r_c all these cross sections are obtained for two different values of r_c , namely, $1.7a_0$ and $2a_0$.

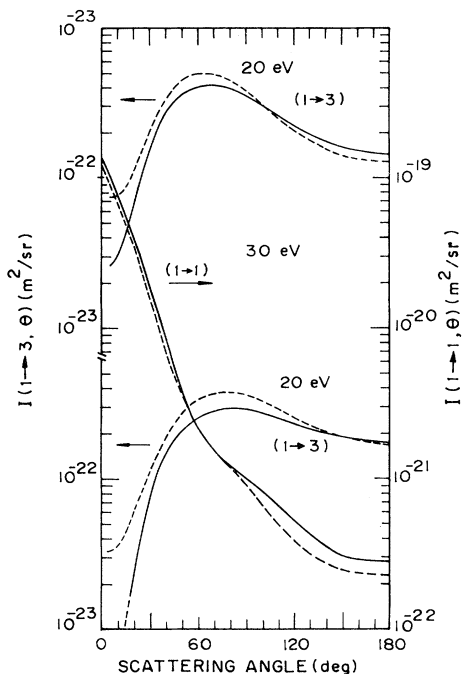


FIG. 1. State-to-state DCS for O_2 vs scattering angles: — — —, present calculation for potential model B with cutoff parameter $r_c = 2a_0$; — — —, the same with $r_c = 1.7a_0$. Left-hand-side ordinate, rotational-excitation cross sections $I(1 \rightarrow 3, \theta)$ at 20 and 30 eV. Right-hand-side ordinates, pure elastic scattering cross sections $I(1 \rightarrow 1, \theta)$ at 30 eV. (Arrows show which scales apply.)

A. Pure elastic and rotational-excitation cross sections

In Fig. 1 we have displayed $I(1 \rightarrow 1, \theta)$ at 30 eV and $I(1 \rightarrow 3, \theta)$ at 20 and 30 eV. As is evident from the curves for $I(1 \rightarrow 3, \theta)$, lowering of cutoff parameter r_c from $2a_0$ to $1.7a_0$ reduces the cross sections over most of the angular range. The situation is just the reverse for the cross sections $I(1 \rightarrow 1, \theta)$. As the energy increases beyond 30 eV, $I(1 \rightarrow 3, \theta)$ gradually shows up a minimum at small angles, and this becomes prominent for $r_c = 2a_0$ (not shown).

Hydrogen is the only molecule for which a few experimental measurements^{5,49} of rotational-excitation cross sections $I(1 \rightarrow 3, \theta)$ are available. Of these the measurements of Srivastava *et al.*⁵ covered the energy interval 3–100 eV. $I(1 \rightarrow 3, \theta)$ at 40 eV measured by these authors shows a broad minimum at small scattering angles (Fig. 2). In a previous study on e - H_2 scattering^{25,26} we computed $I(1 \rightarrow 3, \theta)$ using two different models of long-range potentials. One of these models was used by Hara⁴⁸ (model A, Ref. 26) and the other by Henry and Lane⁵⁰ (model B, Ref. 26). Model A was found to reproduce the shape of the experimentally observed $I(1 \rightarrow 3, \theta)$ at 40 eV quite accurately. Other calcula-

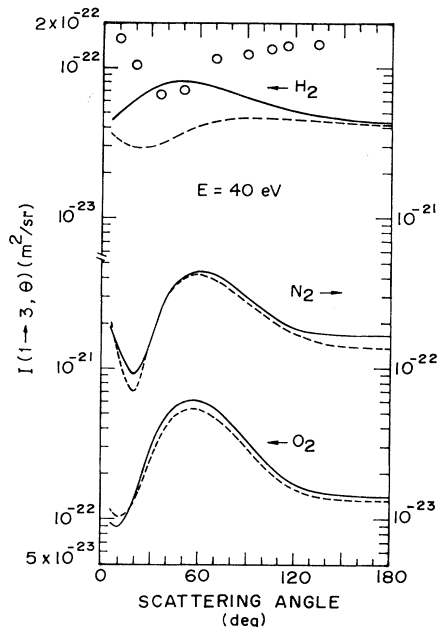


FIG. 2. Rotationally inelastic DCS $I(1 \rightarrow 3, \theta)$ for H_2 , N_2 , and O_2 at 40 eV as a function of scattering angles. H_2 experimental: \circ , Srivastava *et al.* (Ref. 5). H_2 theoretical: — — —, potential model A (Hara), Ref. 26; — — —, potential model B (Henry and Lane), Ref. 26. N_2 and O_2 : — — —, present calculation for potential model A ($r_d = 2a_0$); — — —, present calculation for model B ($r_c = 2a_0$). (Arrows show which scales apply.)

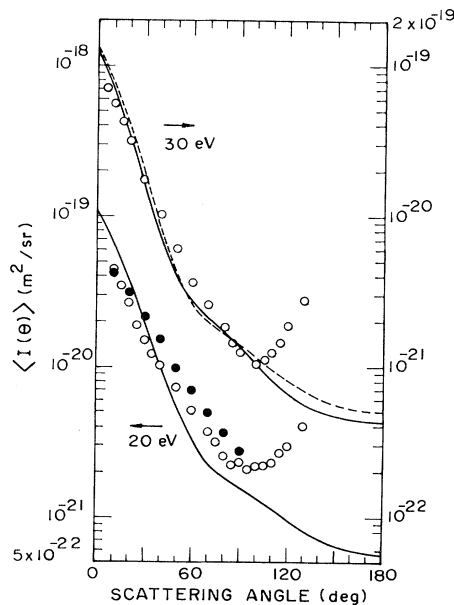


FIG. 3. Average elastic DCS for O_2 at 20 and 30 eV as a function of scattering angles. Experimental: \circ , Wakiya (Ref. 20); \bullet , Trajmar *et al.* (Ref. 18). Theoretical: — — —, present calculation for potential model B with cutoff parameter $r_c = 2a_0$; — — —, the same with $r_c = 1.7a_0$. (Arrows show which scales apply.)

TABLE I. Average elastic differential scattering cross sections (in a_0^2/sr) for $e\text{-O}_2$ scattering (potential model B, $r_c=2a_0$).

E (eV)	20	30	40	50	100	150	200
θ (deg)							
0	38.06	43.76	47.85	51.06	67.12	83.53	97.06
5	30.63	33.76	35.67	36.98	44.61	52.56	57.98
10	23.56	24.82	25.20	25.23	27.52	30.18	30.92
15	17.91	17.88	17.31	16.65	16.22	16.37	15.38
20	13.42	12.61	11.56	10.64	9.370	8.828	7.776
25	9.923	8.709	7.539	6.652	5.590	5.131	4.465
30	7.245	5.922	4.858	4.171	3.640	3.367	3.002
35	5.240	4.003	3.167	2.729	2.620	2.434	2.234
40	3.774	2.735	2.158	1.938	2.006	1.855	1.747
50	2.006	1.439	1.264	1.265	1.234	1.205	1.123
60	1.191	0.965	0.943	0.939	0.821	0.872	0.666
70	0.837	0.760	0.731	0.665	0.651	0.612	0.345
80	0.671	0.615	0.540	0.452	0.564	0.392	0.189
90	0.568	0.485	0.387	0.323	0.474	0.247	0.139
100	0.484	0.376	0.285	0.263	0.378	0.175	0.122
110	0.410	0.294	0.228	0.243	0.294	0.145	0.104
120	0.347	0.239	0.199	0.239	0.232	0.132	0.080
130	0.297	0.203	0.186	0.238	0.191	0.121	0.057
140	0.260	0.181	0.181	0.237	0.166	0.110	0.039
150	0.233	0.169	0.179	0.234	0.152	0.100	0.027
160	0.216	0.162	0.178	0.231	0.144	0.091	0.020
170	0.207	0.158	0.178	0.229	0.140	0.086	0.017
180	0.204	0.157	0.177	0.228	0.139	0.084	0.016

tions,^{26,40,51} including the one²⁶ by the present method using the potential model B (Fig. 2), predicted an opposite angular dependence. To study the dependence of rotational excitation of complex molecules O_2 and N_2 on the form of long-range potentials we have considered the following model potential similar to model A of Ref. 26:

$$\begin{aligned} V_p^0(r) &= \frac{1}{2}\alpha_0(r^2+r_d^2)^{-2}, \\ V_p^2(r) &= \frac{1}{2}\alpha_2r^2(r^2+r_d^2)^{-3}, \end{aligned} \quad (11)$$

where r_d is the cutoff parameter. $V_s^2(r)$ is made to reproduce the correct quadrupole tail by using the expression $Qr^3(r^2+r_d^2)^{-3}$. For both the molecules of oxygen and nitrogen, we have computed $I(1 \rightarrow 3, \theta)$ at 40 eV by using this potential model A ($r_d=2a_0$) and also the model B ($r_c=2a_0$). These are compared on Fig. 2. The cross sections $I(1 \rightarrow 3, \theta)$, for either of the molecules, are found to exhibit the same angular dependence irrespective of the potential model used to calculate them. This angular dependence of $I(1 \rightarrow 3, \theta)$ resembles that for H_2 in the case of potential model A. The nature $I(1 \rightarrow 3, \theta)$ for N_2 remains unaltered throughout the energy interval 20–200 eV (for model B see Fig. 2, Ref. 6; calculations for model A at energies other than 40 eV are not shown). The minima for O_2 is

shallow in comparison with those for N_2 and disappear with decreasing energy (for model B, see Fig. 1; calculations for model A at energies below 40 eV are not shown). Thus at lower energies the shape of $I(1 \rightarrow 3, \theta)$ of O_2 , for either of the models A and B, becomes identical with that of hydrogen molecules for the model B.

B. Average elastic differential scattering cross sections

Average elastic DCS at 20–200 eV for the potential model B ($r_c=2a_0$) are given in Table I. Comparison with available^{18,20} experimental measurements is made in Figs. 3–5. The data of Wakiya²⁰ are reproduced from Figs. 3 and 4 of Ref. 20. The measurements of Trajmar *et al.*¹⁸ are for 20 eV only. We find that the small-angle measurements of Wakiya are in excellent agreement, particularly in shape, with the cross sections computed by us. The best agreement occurs at 50 eV. The deviation is most with the measurements of Wakiya and of Trajmar *et al.* at 20 eV. The present calculations fail to explain the large-angle scattering or the minimum in the observed DCS at and around the scattering angle 90° . We observed these characteristics of the average elastic DCS also for nitrogen molecules⁶ obtained by using the present method. We are unable

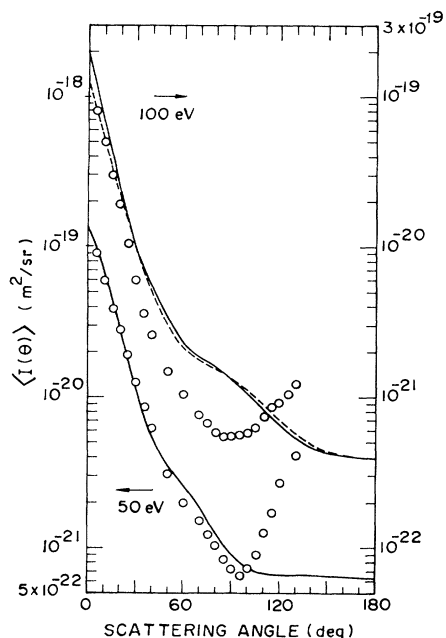


FIG. 4. Average elastic DCS for O_2 at 50 and 100 eV vs scattering angles. Experimental: \circ , Wakiya (Ref. 20). Theoretical: —, present calculation for potential model B with $r_c=2a_0$; - - -, present calculation for potential model A with $r_d=2a_0$. (Arrows show which scales apply.)

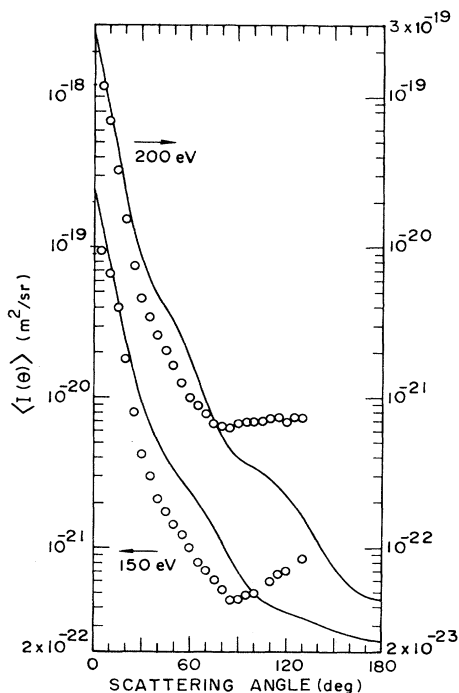


FIG. 5. Average elastic DCS for O_2 at 150 and 200 eV vs scattering angles. Experimental: \circ , Wakiya (Ref. 20). Theoretical: —, present calculation for potential B ($r_c=2a_0$). (Arrows show which scales apply.)

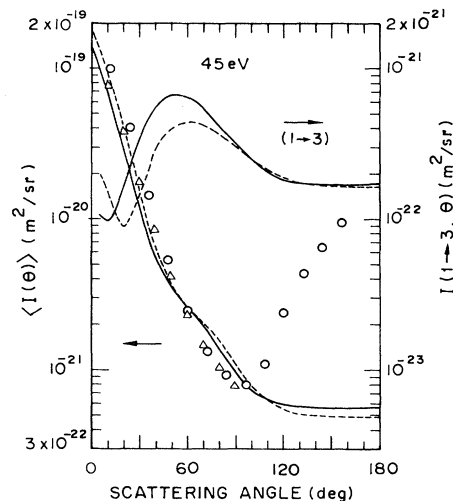


FIG. 6. Comparison of rotational-excitation DCS $I(1 \rightarrow 3, \theta)$ and average elastic DCS $\langle I(\theta) \rangle$ of O_2 with those of N_2 at 45 eV. Experimental: Δ , O_2 cross sections, Trajmar *et al.* (Ref. 18); \circ , N_2 cross sections at 40 eV, Shyn and Carignan (Ref. 52). Theoretical: —, present calculation for O_2 with potential model B ($r_c=2a_0$); - - -, present calculation for N_2 with potential model B ($r_c=2a_0$) of Ref. 6. (Arrows indicate which scales apply.)

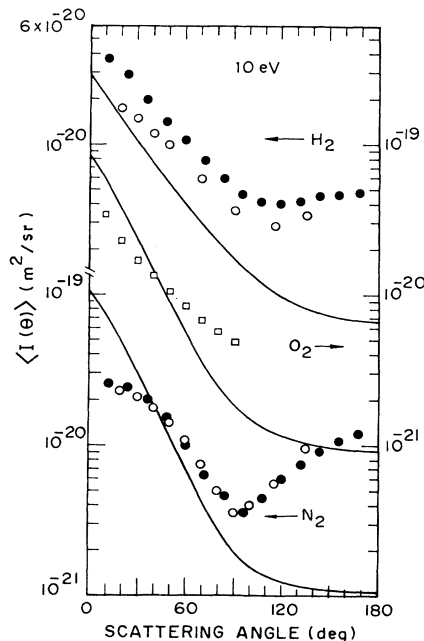


FIG. 7. Comparison of average elastic DCS for H_2 , N_2 , and O_2 at 10 eV. H_2 experimental: \bullet , Shyn and Sharp (Ref. 54); \circ , Srivastava *et al.* (Ref. 53). H_2 theoretical: —, present calculation for potential model B of Ref. 26. N_2 experimental; \bullet , Shyn and Carignan (Ref. 52); \circ , Srivastava *et al.* (Ref. 55). N_2 theoretical: —, present calculation for potential model B ($r_c=2a_0$) of Ref. 6. O_2 experimental: \square , Trajmar *et al.* (Ref. 18). O_2 theoretical: —, present calculation for potential model B ($r_c=2a_0$).

TABLE II. Total cross sections (in a_0^2) for e -O₂ scattering (potential model B).

Energy (eV)	$\sigma(1 \rightarrow 1)^a$	$\sigma(1 \rightarrow 3)^a$	$\langle \sigma \rangle^a$	$\sigma(1 \rightarrow 1)^b$	$\sigma(1 \rightarrow 3)^b$	$\langle \sigma \rangle^b$	$\langle \sigma \rangle^c$
20	24.31	1.01	25.45	22.41	1.22	23.76	28.8
30	21.40	1.28	22.93	19.21	1.40	20.87	
40				17.11	1.47	19.03	
50	17.84	1.61	20.12	15.82	1.66	18.15	20.9
100	16.01	2.87	19.99	14.30	2.85	18.22	
				11.76 ^d	2.74 ^d	15.51 ^d	
150	15.21	3.14	19.25	13.48	3.08	17.44	
200	14.11	2.94	17.70	12.41	2.88	15.91	

^aCutoff parameter $r_c = 1.7a_0$.

^bCutoff parameter $r_c = 2a_0$.

^cExperimental: Trajmar *et al.* (Ref. 18). The datum shown at 50 eV is for 45 eV.

^dObtained with potential model A (cutoff parameter $r_d = 2a_0$).

to compare our results with the theoretical cross sections of Hayashi¹⁴ because these are not given in tabular form. These cross sections are too small at small scattering angles, but they are in better agreement with the observed data at large scattering angles (see Fig. 4, Ref. 20). The reduction of the cutoff parameter to $r_c = 1.7$ increases the cross section for most of the angular region. Calculations for 30 eV are shown in Fig. 3. Use of the potential model A ($r_d = 2a_0$) reduces considerably the cross sections for small scattering angles, but the angular dependence of experimental DCS favors the potential model B. This is evident from a comparison of cross sections predicted by the two models at 100 eV in Fig. 4. We obtained similar results earlier for hydrogen molecules.²⁶

In Fig. 6 a comparison of O₂ cross sections with those of N₂ is made at incident energy 45 eV. The same potential model B and cutoff parameter $r_c = 2a_0$ are used to compute the cross sections.

Measurements of Trajmar *et al.*¹⁸ for O₂ at 45 eV and those of Shyn and Carignan⁵² for N₂ at 40 eV are plotted for comparison. Oxygen cross sections are found to be smaller than the nitrogen ones, the difference being greatest at small scattering angles. Similar results were obtained by Wedde and Strand.¹³ The experimental data confirm this observation. The rotational-excitation cross sections $I(1 \rightarrow 3, \theta)$ of these molecules at 45 eV are also compared in Fig. 6. These cross sections for O₂ are higher than those for N₂ over a considerable range of scattering angles. Finally, a comparison of the behavior of the Glauber cross sections for the molecules H₂, N₂, and O₂, when the incident electron energy falls below the ionization potential of these molecules, is made in Fig. 7. Calculations are performed at 10 eV with potential model B (for N₂ and O₂ we use $r_c = 2a_0$). Recent measurements for hydrogen,^{53,54} nitrogen,^{52,55} and oxygen¹⁸ are plotted for comparison. As is expected the Glauber approx-

TABLE III. Momentum-transfer cross sections (in a_0^2) for e -O₂ scattering (potential model B).

Energy (eV)	$\sigma_m(1 \rightarrow 1)^a$	$\sigma_m(1 \rightarrow 3)^a$	$\langle \sigma_m \rangle^a$	$\sigma_m(1 \rightarrow 1)^b$	$\sigma_m(1 \rightarrow 3)^b$	$\langle \sigma_m \rangle^b$
20	6.54	1.06	7.76	5.99	1.23	7.37
30	4.92	1.19	6.38	4.31	1.22	5.81
40				3.42	1.17	5.10
50	3.49	1.35	5.57	3.04	1.33	5.11
100	2.45	1.96	5.50	2.16	1.90	5.12
				2.15 ^c	1.93 ^c	5.10 ^c
150	1.67	1.60	4.02	1.49	1.55	3.77
200	1.19	1.11	2.72	1.08	1.08	2.57

^aCutoff parameter $r_c = 1.7a_0$.

^bCutoff parameter $r_c = 2a_0$.

^cObtained with potential model A (cutoff parameter $r_d = 2a_0$).

imation fails completely for N_2 and O_2 , while it still predicts the shape of DCS for H_2 .

C. Total and momentum-transfer cross sections

Total cross sections for pure elastic process $J=1 \rightarrow J'=1$ and rotationally inelastic process $J=1 \rightarrow J'=3$ and average total elastic cross sections at energies 20–200 eV are presented in Table II to compare their relative magnitudes. These cross sections are obtained for potential model B with cutoff parameters $r_c=1.7a_0$ and $2a_0$. Calculations for model A ($r_d=2a_0$) at 100 eV are also shown. Comparison is made with the experimental data of Trajmar *et al.*¹⁸ at relevant energies. Momentum-transfer cross sections are given in Table III. When the cutoff parameter r_c is reduced from $2a_0$ to $1.7a_0$ average total elastic cross sections increase by 7 to 11% in the energy interval 20–200 eV. However the rotationally inelastic cross sections decrease at low energies, but they increase at high energies. The results at 100 eV show that the average and pure elastic cross sections for model A are about 18% less than those for model B, while the rotational-excitation cross sections for the two models are almost the same.

Average elastic cross sections calculated by us are found to be in good agreement with the measurements of Trajmar *et al.* (these data will be slightly increased because the large-angle extrapolation used by these authors to compute total cross sections was not correct). We cannot compare our results with the experimental data of Sunshine *et al.* or the theoretical cross section of Myers and of Wedde and Strand (tabulated cross sections are not available). Myers however showed that total rotational-excitation cross sections, which are analogous to $\langle \sigma \rangle - \sigma(1 \rightarrow 1)$ in our nomenclature, were constant ($\sim 0.6a_0^2$) up to an incident energy of 50 eV. We find these cross sections to be energy dependent (for example, our cross sections increase from $1.35a_0^2$ to $2.33a_0^2$ between 20 and 50 eV for potential model B and $r_c=2a_0$).

IV. CONCLUSIONS

For O_2 , unlike H_2 and N_2 , reliable experimental or theoretical average elastic scattering cross sections are not available at intermediate energies. To date, the only experimental data reported are those of Trajmar *et al.*¹⁸ and Wakiya.²⁰ Present cross sections are found to agree well with these, particularly at small scattering angles. In fact, our previous studies on electron-hydrogen²⁶ and electron-nitrogen⁶-molecule scattering suggest that the present Glauber calculations provide moderately accurate elastic scattering data for $e-O_2$ scattering at the energy interval considered here. Of the two potential models considered, the model B cross sections are found to reproduce correctly the shape of elastic cross sections at small scattering angles.

The present method, although simple and elegant, suffers from an inherent limitation: the number of terms actually required for the proper convergence of the one-center expansion (2) are not taken into account. In the effective potential approach this convergence is very important, particularly for complex targets like nitrogen and oxygen. This is evident from the unconverged⁵⁶ and converged⁴¹ close-coupling studies of $e-N_2$ scattering at intermediate energies by Truhlar and co-workers.

Finally, we would like to mention that it is not yet possible, in contrast to electron-atom scattering,^{27,32} to exploit the Glauber amplitude fully for electron-molecule scattering because of the multicenter nature of the problem. The systematic studies of the molecular targets H_2 , N_2 , and O_2 by using the present procedure indicate that the Glauber approximation, if properly utilized, might become an effective tool for our understanding of the electron-molecule scattering problem at intermediate-energy regions.

ACKNOWLEDGMENT

One of the authors (K.K.G.) is thankful to the University Grants Commission, India, for financial support.

¹K. Takayanagi and Y. Itikawa, in *Advances in Atomic and Molecular Physics*, edited by D. R. Bates and I. Esterman (Academic, New York, 1970), Vol. 6, p. 105.

²D. E. Golden, N. F. Lane, A. Temkin, and E. Gerjuoy, *Rev. Mod. Phys.* **43**, 642 (1971).

³N. F. Lane, *Rev. Mod. Phys.* **52**, 1 (1980); P. G. Burke, in *Advances in Atomic and Molecular Physics*, edited by D. R. Bates and B. Bederson (Academic, New York, 1979), Vol. 15, p. 471.

⁴D. G. Truhlar, K. Onda, R. A. Eades, and D. A. Dixon, *Int. J. Quantum Chem. Symp.* **13**, 601 (1979).

⁵S. K. Srivastava, R. I. Hall, S. Trajmar, and A. Chutjian, *Phys. Rev. A* **12**, 1399 (1975).

⁶P. K. Bhattacharyya and K. K. Goswami, *Phys. Rev. A* **26**, 2592 (1982). A good many references on $e-N_2$ scattering are cited in this paper.

⁷J. B. Fisk, *Phys. Rev.* **49**, 167 (1936).

⁸Yu. D. Oksyuk, *Zh. Eksp. Teor. Fiz.* **49**, 1261 (1965) [*Sov. Phys.—JEPT* **22**, 873 (1966)].

⁹K. Takayanagi, *Rep. Ionos. Space Res. Jpn.* **19**, 1 (1965).

¹⁰D. H. Sampson and R. C. Mjolsness, *Phys. Rev.* **144**, 166 (1966).

- ¹¹S. Geltman and K. Takayanagi, *Phys. Rev.* **143**, 25 (1966).
- ¹²E. S. Chang, *Phys. Rev. A* **2**, 1644 (1974).
- ¹³T. Wedde and T. G. Strand, *J. Phys. B* **7**, 1091 (1974).
- ¹⁴S. Hayashi, Ph.D. thesis, University of Tokyo, 1975 (unpublished), as reported in Ref. 20 below.
- ¹⁵H. Myers, *J. Phys. B* **2**, 393 (1969).
- ¹⁶E. Brüche, *Ann. Phys. (Leipzig)* **83**, 1065 (1927).
- ¹⁷C. Ramsauer and R. Kollath, *Ann. Phys. (Leipzig)* **3**, 536 (1929).
- ¹⁸S. Trajmar, D. C. Cartwright, and W. Williams, *Phys. Rev. A* **4**, 1482 (1971).
- ¹⁹J. P. Bromberg, *J. Chem. Phys.* **60**, 1717 (1974).
- ²⁰K. Wakiya, *J. Phys. B* **11**, 3913 (1978).
- ²¹G. Sunshine, B. A. Aubrey, and B. Bederson, *Phys. Rev.* **154**, 1 (1967).
- ²²R. D. Hake, Jr. and A. V. Phelps, *Phys. Rev.* **158**, 70 (1967); A. V. Phelps, *Rev. Mod. Phys.* **40**, 399 (1968); A. Gilardini, *Low-Energy Electron Collision in Gases* (Wiley, New York, 1972), p. 396.
- ²³R. G. Glauber, in *Lectures in Theoretical Physics, Summer Institute for Theoretical Physics, University of Colorado, Boulder, 1958*, edited by W. E. Brittin and L. G. Dunham (Interscience, New York, 1959), Vol. 1, p. 315.
- ²⁴P. K. Bhattacharyya and A. S. Ghosh, *Phys. Rev. A* **12**, 480 (1975).
- ²⁵P. K. Bhattacharyya and A. S. Ghosh, *Phys. Rev. A* **14**, 1587 (1976).
- ²⁶P. K. Bhattacharyya, K. K. Goswami, and A. S. Ghosh, *Phys. Rev. A* **18**, 1865 (1978).
- ²⁷E. Gerjouy and B. K. Thomas, *Rep. Prog. Phys.* **37**, 1345 (1974), and references therein.
- ²⁸C. J. Joachain and C. Quigg, *Rev. Mod. Phys.* **46**, 279 (1974); J. Callaway, *Adv. Phys.* **29**, 771 (1980).
- ²⁹W. Williamson, Jr. and G. Foster, *Phys. Rev. A* **11**, 1472 (1975); G. Foster and W. Williamson, Jr. *ibid.* **13**, 2023 (1976).
- ³⁰R. N. Madan, *Phys. Rev. A* **11**, 1968 (1975); **12**, 2631 (1975).
- ³¹B. K. Thomas and V. Franco, *Phys. Rev. A* **13**, 2004 (1976).
- ³²V. Franco and A. M. Halpern, *Phys. Rev. A* **21**, 1118 (1980).
- ³³A. C. Roy, A. K. Das, and N. C. Sil, *Phys. Rev. A* **23**, 1662 (1981).
- ³⁴A. C. Yates and A. Tenney, *Phys. Rev. A* **5**, 2474 (1972).
- ³⁵T. N. Chang, R. T. Poe, and P. Roy, *Phys. Rev. Lett.* **31**, 1097 (1973).
- ³⁶O. Ashihara, I. Shimamura, and K. Takayanagi, *J. Phys. Soc. Jpn.* **38**, 1732 (1975).
- ³⁷J. T. J. Huang and F. T. Chan, *Phys. Rev. A* **15**, 1782 (1977).
- ³⁸T. T. Gien, *Phys. Lett.* **68A**, 33 (1978).
- ³⁹N. K. Rahman, F. A. Gianturco, and U. T. Lamanna, *Phys. Rev. A* **18**, 74 (1978); F. A. Gianturco, U. T. Lamanna, and N. K. Rahman, *J. Chem. Phys.* **68**, 5538 (1978); F. A. Gianturco, U. T. Lamanna, and S. Salvini, *Int. J. Quantum Chem. Symp.* **13**, 579 (1979).
- ⁴⁰K. J. LaGattuta, *Phys. Rev. A* **21**, 547 (1980).
- ⁴¹K. Onda and D. G. Truhlar, *J. Chem. Phys.* **71**, 5107 (1979); **72**, 5249 (1980).
- ⁴²For a good discussion of the polarization potential, cutoff function, and cutoff parameter see Ref. 4.
- ⁴³N. J. Bridge and A. D. Buckingham, *Proc. R. Soc. London, Ser. A* **295**, 334 (1966).
- ⁴⁴F. H. M. Faisal, *J. Phys. B* **3**, 636 (1970); F. A. Gianturco and D. G. Thompson, *Chem. Phys.* **14**, 111 (1976).
- ⁴⁵D. G. Truhlar, F. A. Van-Catledge, and T. H. Dunning, *J. Chem. Phys.* **57**, 4788 (1972); **69**, 2941(E) (1978).
- ⁴⁶M. L. Cox, Jr. and R. A. Bonham, *J. Chem. Phys.* **47**, 2599 (1967).
- ⁴⁷G. N. Watson, *A Treatise on the Theory of Bessel Functions*, 2nd ed. (Cambridge University Press, Cambridge, England, 1944), p. 366.
- ⁴⁸S. Hara, *J. Phys. Soc. Jpn.* **22**, 710 (1969); M. E. Riley and D. G. Truhlar, *J. Chem. Phys.* **63**, 2182 (1975); **65**, 792 (1976); D. G. Truhlar and N. A. Mullaney, *ibid.* **68**, 1574 (1978); D. Dill and J. L. Dehmer, *Phys. Rev. A* **16**, 1423 (1977); M. A. Morrison and L. A. Collins, *ibid.* **17**, 918 (1978); K. Onda and D. G. Truhlar, *J. Chem. Phys.* **72**, 3460 (1980); J. R. Rumble, Jr. and D. G. Truhlar, *ibid.* **72**, 5223 (1980); S. Sur and A. S. Ghosh, *Phys. Rev. A* **25**, 2519 (1982).
- ⁴⁹H. Ehrhardt and F. Linder, *Phys. Rev. Lett.* **21**, 419 (1968); F. Linder and H. Schmidt, *Z. Naturforsch.* **A26**, 1603 (1971); G. Joyez, J. Comer, and F. H. Read, *J. Phys. B* **6**, 2427 (1973).
- ⁵⁰R. J. W. Henry and N. F. Lane, *Phys. Rev.* **183**, 221 (1969).
- ⁵¹D. G. Truhlar and M. A. Brandt, *J. Chem. Phys.* **65**, 3092 (1976).
- ⁵²T. W. Shyn and G. R. Carignan, *Phys. Rev. A* **22**, 923 (1980).
- ⁵³S. K. Srivastava, A. Chutjian, and S. Trajmar, *J. Chem. Phys.* **63**, 2659 (1975).
- ⁵⁴T. W. Shyn and W. E. Sharp, *Phys. Rev. A* **24**, 1734 (1981).
- ⁵⁵S. K. Srivastava, A. Chutjian, and S. Trajmar, *J. Chem. Phys.* **64**, 1340 (1976).
- ⁵⁶M. A. Brandt, D. G. Truhlar, and F. A. Van-Catledge, *J. Chem. Phys.* **64**, 4957 (1976).